

# BESS at Point of Common Coupling for Wind Farm

Sandeep Tapre<sup>1</sup> and K. Venkata Ramamohan<sup>2</sup>

<sup>1</sup>M.E (Student) MSS's College of Engg. Jalna

<sup>2</sup>MSS's College of Engg. Jalna

E-mail: <sup>1</sup>sandeep.tapre85@rediffmail.com, <sup>2</sup>ram.mohan822@gmail.com

---

**Abstract**—A computational procedure to determine the Battery energy storage system capacity and the evaluation of the voltage. This paper presents the results of a wind data and provide effectively continuous power for the consumers or grid without any disturbance. It also examined for the purpose of attenuating the effects of unsteady input power from wind farms. A novel 2 wind generating plants at Point of common coupling, Battery storage-based power allocation method also is proposed. The effectiveness of these methods was verified using MATLAB/SIMULINK software.

## 1. INTRODUCTION

Wind power is the fastest-growing renewable energy source, but one of the typical problems of wind energy converters (WECs) is the variation in their delivered power, which is the main cause of the relationship between the random nature of wind and the power. The purpose of the present investigation is to fill in the gap in the aforementioned daily load-tracking application. It addresses the design of a BESS, incorporated into a power buffer for the wind farm. While the BESS possesses higher energy capacity than several other energy storage media, and hence, it is suitable for the long-term load-tracking operation [1], BESS is also shown to be cost-effective for use in power systems [2]. However, nowadays it is common to find wind converters where an electronic converter is used to connect the generator to the network, so the delivered power can be smoothed [3].

The purpose of this paper is to investigate the periodic power pulsations that have been measured during the day and give continuous power. The loads on an electricity supply system, which are reflected in the spot price of electricity, vary according to the time of day, day of the week, season, and also other, unpredictable factors. For the wind farm application, for example, a flow battery system has been described in [4], although the authors have yet to provide a method by which the battery capacity can be determined. Thus, the present investigation proposes a methodology to determine the required BESS capacity for the purpose of daily load tracking or load leveling. The method is based on a given wind power profile and the optimization of an objective function through

which the Optimal dispatched power level from the wind farm will be obtained.

## 2. MODEL DESCRIPTION

This paper is organized as follows. PMSG is interconnected with the grid through a fully rated converter so that the variable ac frequency at the generator terminal is converted to steady grid frequency at the output. Here two plants are to be considering which are join at PCC through the PWM Generator as shown in Fig 1. Also it shows that the wind energy captured by the turbine blades is converted through the PMSG into electrical power, denoted by  $P_w$ . From previous references, it is clear that  $P_w$  tends to be highly stochastic, and an effective way to describe  $P_w$  could be through statistical means [5], [6]. Alternatively, as part of the wind farm planning, site selection, and design process, wind data are often collected at site if such data of (say) past few years are unavailable. As the main focus of this paper is on the design of the BESS, it is now assume that sufficient wind data are available and the profile of  $P_w$  is known over a period of  $T$  h. Fig. 2 shows a typical profile of  $P_w$ , derived from the wind speed data. In the figure,  $P_w$  has been normalized, and hence is within the range [0, 1] per unit (p.u.).

All wind speed distributions were corrected to a long-term mean wind speed of 12 m/s. At short time scales. As per Fig. 1 the system configuration of a direct drive PMSG based grid interfaced WECS. A horizontal axis wind turbine is used to drive the PMSG. A surface mounted non salient pole type PMSG is used. The kinetic energy presents in the wind is converted into the mechanical torque using a wind turbine. Mechanical energy is converted into electrical energy using a PMSG. To facilitate variable speed operation for achieving MPPT, the PMSG cannot be interfaced with the grid directly. Therefore, two VSCs are used in back to back configuration with common DC link known as a MSC and a GSC. These VSC's are controlled independently.

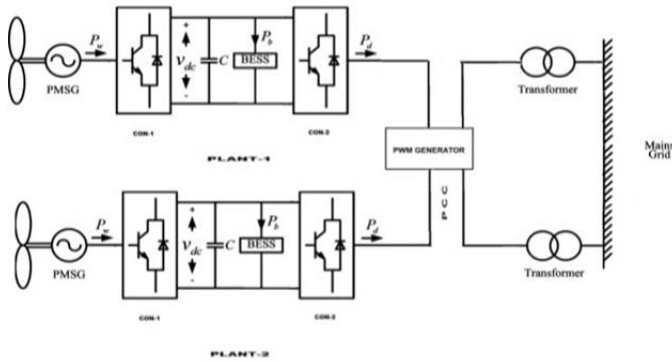


Fig. 1: Variable speed wind turbine with interconnection to the mains grid through BESS.

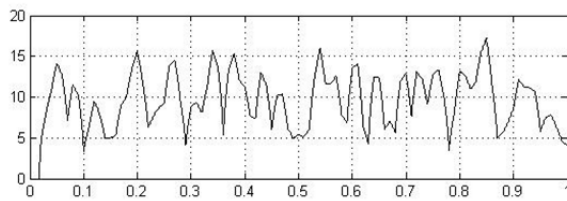


Fig. 1: Typical wind power profile based on data taken: constant Pd is shown.

One can assume that the power loss in the two converters is negligible. The dc-link capacitor C functions as harmonics filter, and in some designs, it can also take the role of the energy-storage system [7]. However, typical energy storage capacity of the capacitor tends to be small compared to the BESS considered in the study. Hence, in terms of initial power flow analysis, the capacitor power may be neglected. It is further assumed that the dispatched power Pd from CON2 to the mains grid is to be kept constant over the interval T. Although this assumption tends to facilitate analysis, it also has a desirable effect from a practical viewpoint: it prevents the fluctuating Pw from impacting negatively on the grid, in terms of network voltage and frequency profiles. To realize the constant power feature, the mismatch power between Pw and Pd has to be compensated for by the BESS, which has the output Pb (t), shown in Fig. 1.

### 3. CONTROL ALGORITHM

The block diagram of the proposed control scheme as in Fig. 1, The MSC controls the active power of the PMSG to achieve MPPT and the GSC regulates the DC link voltage under change in active power output from the PMSG. The control scheme for the MSC and the GSC are as follows:

#### 3.1 Machine Side Converter (MSC) Control

The MSC is controlled in rotor reference frame and the phasor diagram. The stator resistance of a PMSG is negligible which is practically valid in MW size of generators. The rotor flux

linkage is aligned with the d-axis of the synchronous reference frame. All vectors along with dqaxis frame rotate in space at synchronous speed ωs which is also the rotor speed of the generator ωr. The stator current vector is perpendicular to the rotor flux vector λr.

#### 3.2 Mathematical model

The following table shows the definition of various variables used in this model:

E = Kinetic Energy (J)

P = Density (kg/m<sup>3</sup>)

M = Mass (kg) A = Swept Area (m<sup>2</sup>)

V = Wind Speed (m/s)

Cp = Power Coefficient

P = Power (W)

r = Radius (m)

Under constant acceleration, the kinetic energy of an object having mass m and velocity v is equal to the work done W in displacing that object from rest to a distance s under a force F i.e.

$$E = W = Fs$$

According to Newton’s Law, we have:

$$F = ma$$

Hence,

$$E = \text{mass} \dots (1)$$

Using the third equation of motion:

$$P_M = \frac{1}{2} \rho A v_W^3 C_P (1)$$

$v^2 = u^2 + 2as$  and as per paper [10].

A German physicist Albert Betz concluded in 1919 that no wind turbine can convert more than 16/27 (59.3%) of the kinetic energy of the wind into mechanical energy turning a rotor. To this day, this is known as the Betz Limit or Betz’Law. The theoretical maximum power efficiency of any design of wind turbine is 0.59 (i.e. no more than 59% of the energy carried by the wind can be extracted by a wind turbine). This is called the “power coefficient” and is defined as:

$$C_{pmax} = 0.59$$

Also, wind turbines cannot operate at this maximum limit. The Cp value is unique to each turbine type and is a function of wind speed that the turbine is operating in. Once we incorporate various engineering requirements of a wind turbine - strength and durability in particular – the real world limit is well below the Betz Limit with values of 0.35-0.45

common even in the best designed wind turbines. By the time we take into account the other factors in a complete wind turbine system - e.g. the gearbox, bearings, and generator and so on - only 10-30% of the power of the wind is ever actually converted into usable electricity. Hence, the power coefficient needs to be factored in equation (4) and the extractable power from the wind is given by:

$$P_{avail} = \frac{1}{2} \rho A v_w^3 C_p \quad (2)$$

Where  $\rho$  is the air density which is approximately equal to 1.2 kg/m<sup>3</sup> this study; where  $C_p$  is the power coefficient considered 0.48 for this wind turbine;  $A$  is the sweep area of turbine blades in m<sup>2</sup> and  $v_w$  is the wind velocity in m/s. In direct drive system, due to the absence of a gear box, the mechanical torque (TM) and the shaft speed of the wind turbine are directly transferred to the shaft of the generator. The mechanical torque developed by the wind turbine is as,

$$T_m = P_m / \omega_m \quad (3)$$

### 3.3 Grid Side Converter (GSC) Control

The DC link voltage is selected such that it should be more than peak of the line voltage for satisfactory operation of GSC for controlled active power transfer to the grid.

### 4. BESS CAPACITY

The battery capacity is normally specified in terms of power and energy capacity [9]. The energy capacity describes the energy that can be drawn from or stored in the battery. The power rating determines the power that can be supplied or stored by the battery under rated discharge/charge time interval. The capital cost of the battery can also be determined, based on the power and energy capacities [8]. Consequently, the design problem in hand is to determine the BESS capacity based on a cost-benefit consideration, as shown later.

In the buffer system, the BESS power  $P_b(t)$  can be written in terms of  $P_w$  and  $P_d$  as

$$P_b(t) = P_w - P_d \quad (4)$$

From (1), for a given constant  $P_d$ ,  $P_b(t)$  will vary in the same manner as  $P_w$ . By setting  $P_d$  to another constant value will only result in the  $P_b(t)$  curve being shifted up or down, but  $P_b(t)$  will remain as the same shape as  $P_w$ . For example, for the  $P_w$  profile given in Fig. 2, the  $P_b(t)$  profile given in Fig. 3(a) corresponds to  $P_d = 0.6$  p.u. From Fig. 3(a), one finds that the maximum battery power  $P_{b,max}$  occurs at  $T_1$  when  $P_{b,max} = -0.5$  p.u. over the interval  $T$ . The negative sign indicates that, at this precise moment, the BESS is discharging. It is quite conceivable for a different value of  $P_d$ , the corresponding  $P_{b,max}$  may be positive.

It then indicates that the BESS is being charged at the maximum value at that instance. Integration of  $P_b(t)$  with respect to time yields the net energy ( $E_b$ ) injected into or discharged from the BESS, up to time  $t$ . Corresponding to the changes in  $P_b(t)$ , the  $E_b(t)$  profile will also vary for different  $P_d$ . For instance,  $E_b(t)$  profiles corresponding

to  $P_d = 0.55, 0.6$ , and  $0.65$  p.u., respectively, have been given in Fig. 3(b). Positive values in Fig. 3(b) show net gain/loss in stored energy in the BESS, as compared to the battery initial stored energy level. For specific value of  $P_d$ , the corresponding value of  $P_{b,max}$  determines the BESS power capacity. To achieve the goal of dispatching the constant  $P_d$  over the designed period  $T$ , the BESS capacity has to be specified to be at least as large as the

corresponding  $P_{b,max}$ . once the BESS capacity is designed to be at least as large as  $P_{b,max}$ , the BESS could absorb/supply the surplus/shortfall in power for the corresponding constant dispatched level  $P_d$ . As described earlier, besides the power capacity, the battery energy capacity should also be considered. For the study undertaken in this paper, the BESS energy capacity is specified in a similar manner as in the case of BESS power capacity: the energy capacity of the BESS has to be as large as that it could absorb/supply the maximum amount of the charged/discharged energy. Hence, the BESS energy capacity should be at least as large as  $E_{b,max}$  for the corresponding  $P_d$  value.

Fig. 2: Simulink model for BESS at point of common coupling at wind farm with interconnection to the Loads.

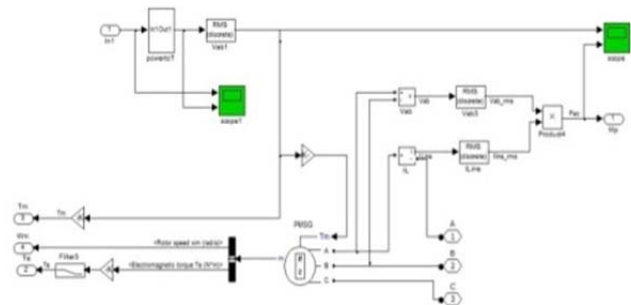


Fig. 3: Simulink model for PMSG

### Determination of BESS Power and Energy Capacities

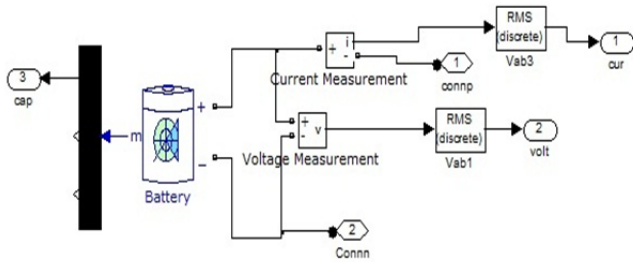


Fig. 4: Simulink model for BESS

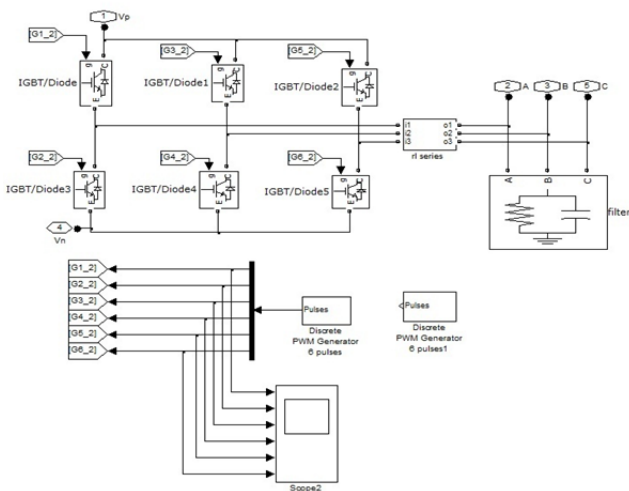


Fig. 5: Simulink model for Converter

5. SYSTEM CONFIGURATION

5.1 Battery Model

Several equivalent battery circuit models have been reported in the literature. The models are applicable to study the battery behavior over short- or long-term intervals during its charge/discharge process [16]. For the present study, the consideration is for the charging/discharging processes of the battery for relatively long-term operations, e.g., over hours/days. The lead-acid battery model proposed by Ceraolo [17] is suitable for such an application.

5.2 Capacitor used

Characteristics

1. Rated capacitance 100-2000  $\mu$ F
2. Capacitance tolerance = 10%
3. Rated DC Voltage ( $U_n$ ) max 1800 V DC
4. Self-inductance max. 70 nH
5. Typical tan. d (50 Hz)  $< 5.0E-4$
6. Series resistance  $< 3 \text{ m}\Omega/1 \text{ kHz}$
7. Filling Resin Dry, UL94, V0
8. Dielectric Self healing MPP aluminium case without overpressure device

9. Terminals M6, M8 internal threads M8 screw type's bolts
10. Maximum rating :- Overvoltage  $1.1 \times U_n$  (8h/day)
11. Max. (dV/dt) 25 V/us

5.2 Application

- I. Hybrid vehicles
- II. Wind plants
- III. Solar power plants
- IV. Electric energy generation from sea waves
- V. Medical equipment
- VI. Industrial equipment
- VII. Car electronics
- VIII. Railway and turbines (generator)
- IX. Frequency transducer
- X. Elevators

6. SYSTEM OUTPUTS

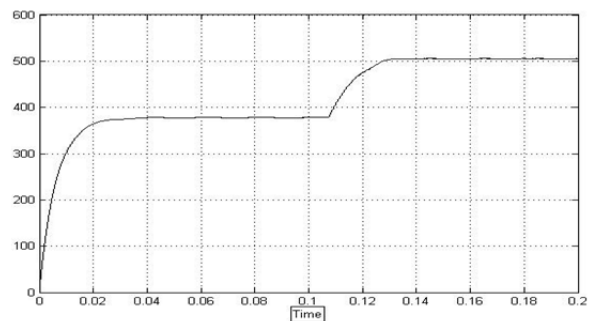


Fig. 6: Graph for Capacitor charging (Voltage v/s Time)

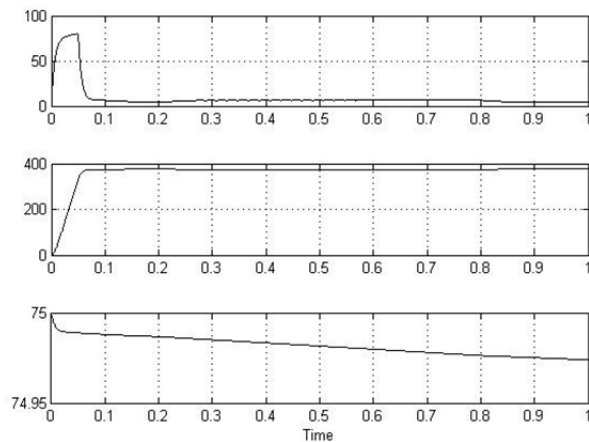


Fig. 7: Graph for SOC for Battery charging & discharging

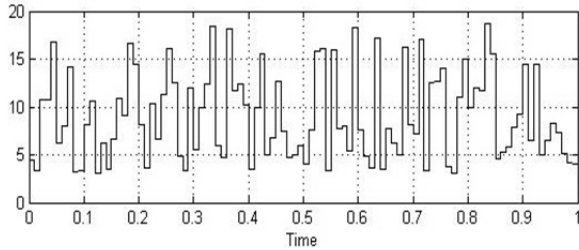


Fig. 8: Graph for Power generating in MW

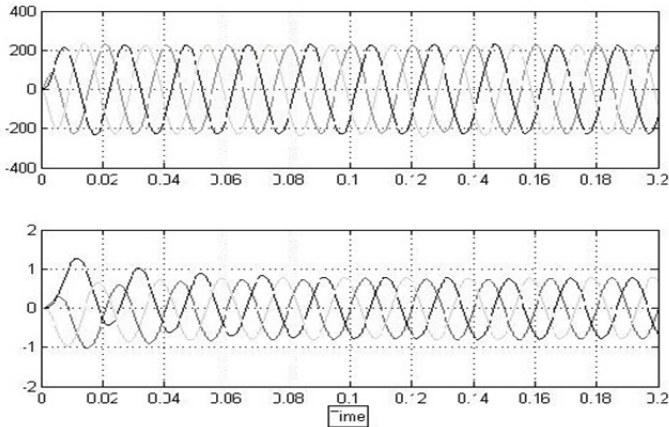


Fig. 9: Graph for Converter output (voltage & current)

## 7. CONCLUSION

This research has established that key aspects of the use of Energy storage can be captured by a simplified probabilistic approach, which requires only limited input data. Specific conclusions based on the modeling indicate the following:

A method to determine the BESS capacity has been developed with the purpose of not only keeping the injected power from the wind farm constant, but also to achieve maximum economic benefit.

The proposed BESS and capacitor sizing procedure has been demonstrated through simulation studies and using the wind data obtained from a theoretically wind farm

Energy storage up to one day cannot exclude energy curtailment in a weak grid connection.

Energy management incorporating energy storage over

24 hrs and energy curtailment can allow up to three times the amount of wind energy to be absorbed by a weak grid compared to conventional grid connection of wind farms. The impact of energy capacity has been sidestepped in this study through the assumption of a storage capacity that is large enough for the time scale considered. Nevertheless, the conclusions should be valid provided reasonably generous storage capacities are used of the orders of magnitude estimated.

## REFERENCES

- [1] J. P. Barton and D. G. Infield, "Energy storage and its use with intermittent renewable energy," *IEEE Trans. Energy Convers.*, vol. 19, no. 2, pp. 441–448, Jun. 2004.
- [2] P. F. Ribeiro, B. K. Johnson, M. L. Crow, A. Arsoy, and Y. L. Liu, "Energy storage systems for advanced power application," in *Proc. IEEE*, vol. 89, no. 12, pp. 1744–756, Dec. 2001.
- [3] C. Carrillo, "Análisis y simulación de sistemas eólicos aislados," Ph.D. dissertation (in Spanish), Universidade de Vigo, Spain, 2001.
- [4] T. Hennessy and M. Kuntz, "Flow battery storage application with wind power," in *Proc. IEEE PES Transmiss. Distrib. Conf. Expo.*, Dallas, May 2006, pp. 937–939.
- [5] R. Karki, P. Hu, and R. Billinton, "A simplified wind power generation model for reliability evaluation," *IEEE Trans. Energy Convers.*, vol. 21, no. 2, pp. 533–540, Jun. 2006.
- [6] G. Sideratos and N. D. Hatzigiorgiou, "An advanced statistical method for wind power forecasting," *IEEE Trans. Power Syst.*, vol. 22, no. 1, pp. 258–265, Feb. 2007.
- [7] W. Li, G. Joos, and C. Abbey, "Attenuation of wind power fluctuations in wind turbine generators using a dc bus capacitor based filtering control scheme," in *Proc. IEEE 41st IAS Annu. Meet.*, Florida, Oct. 2006, pp. 216–220.
- [8] T.-Y. Lee and N. Chen, "Optimal capacity of the battery energy storage system in a power system," *IEEE Trans. Energy Convers.*, vol. 8, no. 4, pp. 667–673, Dec. 1993.
- [9] J. N. Baker and A. Collinson, "Electrical energy storage at the turn of the millennium," *Inst. Elect. Eng. Power Eng. J.*, vol. 13, no. 3, pp. 107–112, Jun. 1999.
- [10] S. Mathew, *Wind Energy, Fundamentals, Resource Analysis and Economics*. Berlin, Germany: Springer-Verlag, 2006.
- [11] S. Heier and R. Waddington, *Grid Integration of Wind Energy Conversion Systems*, 2nd ed. Hoboken, NJ: Wiley, 2006.
- [12] C. Luo and B.-T. Ooi, "Frequency deviation of thermal power plants due to wind farms," *IEEE Trans. Energy Convers.*, vol. 21, no. 3, pp. 708–716, Sep. 2006.
- [13] C. Carrillo, A. E. Feijoo, J. Cidras, and J. Gonzalez, "Power fluctuations in an isolated wind plant," *IEEE Trans. Energy Convers.*, vol. 19, no. 1, pp. 217–221, Mar. 2004.
- [14] S. Nomura, Y. Ohata, T. Hagita, H. Tsutsui, S. Tsuji-Iio, and R. Shimada, "Wind farms linked by SMES systems," *IEEE Trans. Appl. Supercond.*, vol. 15, no. 2, pp. 1951–1954, Jun. 2005.